J Mater Sci (2018) 53:5584–5603

Interface Behavior

A review of slip transfer: applications of mesoscale techniques

Abigail Hunter[1,*], Brandon Leu[2], and Irene J. Beyerlein[2]

[1] Los Alamos National Laboratory, P.O. Box 1663, MS T086, Los Alamos, NM 87545, USA
[2] University of California, Santa Barbara, Engineering II Building 1355, Santa Barbara, CA 93106-5050, USA

Received: 29 August 2017
Accepted: 21 November 2017
Published online: 1 December 2017

ABSTRACT

In this review article, we present and discuss recent mesoscale modeling studies of slip transmission of dislocations through biphase interfaces. Specific focus is given to fcc/fcc material systems. We first briefly review experimental, atomistic, and continuum-scale work that has helped to shape our understanding of these systems. Then several mesoscale methods are discussed, including Peierls–Nabarro models, discrete dislocation dynamics models, and phase field-based techniques. Recent extensions to the mesoscale mechanics technique called phase field dislocation dynamics are reviewed in detail. Results are compiled and discussed in terms of the proposed guidelines that relate composite properties to the critical stress required for a slip transmission event.

Introduction

Nanolayered (NL) composites, consisting of two or more dissimilar phases, have great potential to achieve many outstanding structural properties simultaneously. Initially, many earlier works were motivated to reach exceptionally high strengths with these materials [37, 44, 65, 67, 80, 86]. However, in more recent years, they have been shown to possess not only enhanced strength but also better stability in harsh environments than is possible with their coarser-grained composite counterparts [13, 19, 68, 70, 104].

The constituents of NL composites are polycrystalline materials that, under an applied strain, deform by the motion of dislocations. They owe much of their high strength to the ability of the biphase interfaces to hinder the glide of dislocations through the phases. Dislocations usually move in arrays, containing many seemingly identical dislocations, gliding on the same plane or closely spaced neighboring parallel planes. When a dislocation or dislocation array meets a boundary, it can no longer continue to glide. To transmit slip across the bimetal interface a series of events needs to occur, starting with the absorption of the dislocations into the interface. The disturbance in the structure of the interface caused by the newly absorbed dislocations can trigger nucleation of a dislocation into the adjoining crystal. This sequence of events is collectively called slip transmission (Fig. 1). The same dislocation has not actually transmitted in slip transmission, but the action of slip has been transmitted. The critical stress that must be overcome for slip transmission is referred to as a critical transmission stress τ_{crit}. Its value is relatively

Address correspondence to E-mail: ahunter@lanl.gov

https://doi.org/10.1007/s10853-017-1844-5

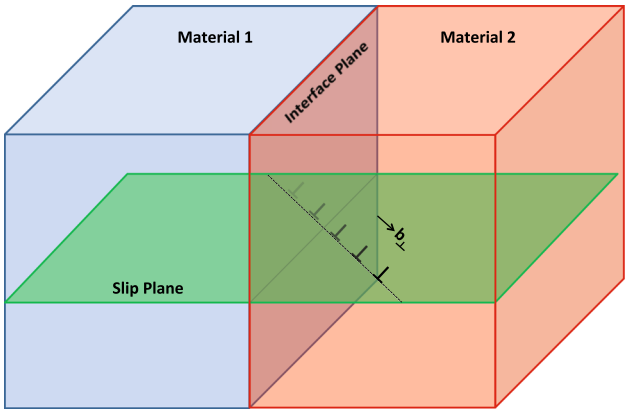

Figure 1 Schematic representation of a slip transmission event.

large compared to that for dislocation glide in the phases, and hence, the strength of the NL composite can be related to τ_{crit}.

Slip transmission can occur across the grain boundaries and biphase interfaces in coarse-grained polycrystalline materials (with crystals bearing diameters in the tens to hundreds of microns), but its contribution toward strength is much greater in nanocrystalline materials (with crystal diameters on the order of 100 nm or less). In large-grained materials, slip transmission across a boundary is enabled by the development of dislocation pile-ups at the boundary (or interface). The first (or lead) dislocation of the pile up, facing the boundary, experiences the greatest stress concentration and, therefore, requires the least applied work to overcome τ_{crit}. When the grains in the layers (or the layer thickness) become sufficiently fine that only a single dislocation can travel through the grain at a time, then more applied work is required to enable the lone dislocation to overcome the same value of τ_{crit}. In NL composites with layer thicknesses on the order of tens of nanometers, it would be expected that the number of dislocations in the array contains one to a few dislocations. Hence, τ_{crit} would be the primary material variable determining the limit of strength in NL materials.

Many experimental studies have helped to identify the primary interface characteristics that govern τ_{crit} for grain boundaries [15, 21, 50, 51, 98] and bimetal interfaces [14, 57, 59, 75, 78, 81, 91, 93, 94]. These analyses were primarily structured around the geometric criteria of Werner and Prantl [98], Lee–Roberston–Birnbaum (LRB) [50, 51], and Clark et al. [21], which favors slip transmission to/from slip systems that are well aligned across the interface. Better alignment results in a smaller value for the Burgers vector of the residual dislocation left in the interface after a transmission event [56, 59, 66]. Transmission may also be aided by high resolved shear stresses at the boundary that are sufficient to push dislocations into the interface from one side and nucleate them out of the other side [50, 51, 66].

Compared to grain boundaries, bimetal (heterophase) interfaces seem to require much higher stresses for slip transmission [99, 100]. Bimetal NL composites can achieve much higher strengths and hardnesses than their nanocrystalline counterparts bearing the same crystalline size scales (grain size versus layer thickness) due to high densities of bimetal interfaces. Generally, for these NL composites, "smaller is stronger," as demonstrated via hardness measurements [65, 68, 80, 86] and in a some cases strength measurements [37, 60, 70, 71]. Among the same bimetal systems, the defect structure of the interface can affect its ability to block slip transfer and in turn, strength. In multilayer deposited films containing low-energy interfaces formed after deposition, slip transfer appeared to prevail only at the very finest nanolayer thicknesses (2–5 nm), when sufficiently high stresses are achieved [67]. However, for bimetal sheets fabricated by a metal forming technique called accumulative roll bonding (ARB) [19, 72] containing interfaces with a distinctly different interface structure and energy, slip transfer can occur at larger length scales, suggesting that slip transfer is easier in ARB NLs compared to the deposited films.

Many of the detailed mechanisms involved in the transfer of slip across boundaries are challenging to directly observe experimentally. To aid in understanding, several numerical studies have been carried out to simulate slip transmission in bimetal interfaces with an emphasis on applications to fcc/fcc or fcc/bcc systems [10, 33, 47, 69, 74, 90, 91, 103]. These systems were usually simulated either at the atomic-scale, through molecular dynamics (MD) simulations, or the continuum-scale, treating the material as a homogeneous continuum [10, 33, 47, 69, 74, 90, 91, 103]. Some works have treated the mesoscale, but these works are typically concerned with crystallographic relationships between slip systems across an interface or boundary and hence are largely based on geometry. Taken together, these studies over this broad range of length scales have contributed to understanding

certain aspects of the problem of slip transmission across a biphase interface.

In this review article we discuss and compile recent activity in mesoscale modeling efforts directed toward modeling slip transmission across biphase interfaces. We begin by briefly reviewing continuum-scale and atomistic methods for addressing slip transfer across biphase boundaries ("Analytical elastic approaches for modeling slip transfer" and "Atomistic simulations addressing slip transfer" sections, respectively). From this work, several general guidelines on the relationship between intrinsic material parameters and the stress required for transmission have emerged, and these are presented in the "Guidelines for slip transfer" section. We focus the majority of this article on mesoscale modeling techniques that have previously demonstrated value and future potential in helping to bridge some gaps in the understanding of deformation mechanisms operating at intermediate scales, that is, above the atomistic scale and below the continuum-scale. Mesoscale modeling of slip transmission across biphase interfaces is discussed in detail starting in the "Mesoscale mechanics simulations of slip transfer" section. This will include recently published developments in Peierls–Nabarro (PN) models, discrete dislocation dynamics (DDD) modeling, and phase field (PF)-based techniques. We then follow with a review of the phase field dislocation dynamics (PFDD) formulation [11, 102] and recent advances to include the image fields due to a mismatch in moduli across the interface ("Phase field dislocation dynamics (PFDD)" section). As done with other approaches, this capability was first demonstrated on modeling dislocation interactions with a coherent Cu–Ni interface [102]. These results along with others reported in the literature are presented and compared in the "The Cu–Ni bicrystal system" section. Following this, in the "Extending to other fcc/fcc systems" section, we extend the discussion to include results from several fcc/fcc systems, making comparisons to experimental and numerical data reported in the literature when possible. We then discuss key findings related to understanding the variables that govern transitions from full dislocation slip to partial dislocation slip and deformation twinning in nanosized fcc crystals. Such studies help define the dominant deformation mechanisms active for a given material and loading condition, and determine the impact of such transitions on the macroscopic stress–strain response. Finally, we conclude with a discussion of problems worth addressing, such as alternate crystal structures (bcc or hcp metals) and heterogeneous material systems, which includes both free surface and voids, and phase transformations.

Analytical elastic approaches for modeling slip transfer

Continuum models for slip transmission across biphase interfaces have played an important role determining the key aspects, such as image forces due to moduli mismatch, misfit strain fields due to lattice mismatch, and effect of the residual dislocation that has been left behind following slip transmission. Early continuum mechanics models studied the effect of image forces on τ_{crit} [69, 74] by predicting the stress fields on dislocations within a few Burgers vectors from the interface. The interfaces modeled were nearly coherent so that the lattice mismatch and resulting misfit strains were negligible. In two-phase bimaterial systems, the difference in line energy of the dislocation between the two phases can cause an asymmetry in τ_{crit}, such that dislocations prefer to transmit to the material with the lower line energy. By considering the stress state when a dislocation interacts with these image forces, Koehler estimated the stress required to move the dislocation to the interface against these forces [44] and then argued that the τ_{crit} for a dislocation to transmit would scale in the same way.

Guidelines for slip transfer

For several decades, models have been developed that provide general guidelines on the relationship between intrinsic material parameters and the transmission stress between dissimilar metals. A series of dislocation mechanics models focused on the effect of elastic moduli mismatch [7, 47, 74]. This aspect leads to an asymmetry in the transmission stress, in which the transmission stress differs depending on which material the dislocation originates and to which it transmits. The moduli mismatch generates image forces at the interface that attract a dislocation to the interface if it lies in the material with the larger modulus and repels it if it lies in the material with the smaller one. One of the first models of this type was developed by Head [32], who additionally considered the distance between the dislocation and the

interface, c'. The critical transmission stress τ_{crit} for the transmission of a screw dislocation from the softer material was proposed to scale as

$$\tau_{crit} \approx -\frac{(G_2 - G_1)G_1}{2\pi(G_2 + G_1)c}, \quad (1)$$

where $c = 2/bc'$ is a non-dimensional distance from the interface following [74], and G_1 and G_2 is the shear modulus in the donor material (material 1) and the recipient material (material 2), respectively. However, because Head considered a Volterra dislocation, for small values of c, τ_{crit} increases without bound resulting in a singularity as the dislocation meets the interface. This was noted by Dundurs [24] who suggested that this is due to the idealization of a singular dislocation within the formulation.

Shortly thereafter, a model by Pacheco and Mura [74] was developed that built upon the Peierls model [76] for a continuously distributed dislocation rather than a Volterra dislocation. According to this model, τ_{crit} for the transmission of a screw dislocation that transmits from the material of lower to higher modulus scales as

$$\tau_{crit} \approx -\frac{(G_2 - G_1)G_1}{G_2 + G_1}\left(\frac{1}{c^2 + 1} + \frac{\tan^{-1} c}{c}\right), \quad (2)$$

where for sufficiently large c, we retrieve the same scaling in the shear moduli as initially presented by Head [32]. Differences between the two models are most notable when the dislocation is approximately three lattice spacings or less from the interface [74]. Similarly, Koehler [44] also concentrated on modulus mismatch and retrieved a similar relationship to calculate the τ_{crit} needed to transmit a screw dislocation starting in the softer material

$$\tau_{crit} \approx \frac{(G_2 - G_1)G_1 b}{4\pi(G_2 + G_1)c'}, \quad (3)$$

where b is the Burgers vector magnitude. Koehler also predicted a weak dependence of the image forces on the character of the dislocation, which is not explicitly included in the relationship shown in Eq. 3. Furthermore, he found that when a full dislocation splits into partials, the elastic repulsion of partial dislocations may be significantly reduced because the leading partial and trailing partial are not equally repelled by the image forces. Thus, when choosing the softer material, one should also consider materials which have perfect dislocations or higher intrinsic stacking fault energies. Hence, the stacking fault energy may be an important consideration in developing general guidelines to predict transmission stresses because it determines the relative ease with which a dislocation may split into partials. This idea is supported by more recent work from Xin and Anderson [7], who found that when the unstable stacking fault energy on the slip planes is reduced so is τ_{crit}.

Krzanowski [47] pursued a sightly different approach considering the transmission of a Volterra dislocation across a diffuse interface, with an elastic shear modulus that varies linearly over a finite interface width w,

$$\tau_{crit} \approx \frac{(G_2 - G_1)b}{4\pi w}\ln\frac{w}{2b}. \quad (4)$$

This suggests that interfaces are strong barriers to slip transmission when the interfaces are chemically sharp with large, abrupt changes in elastic moduli. τ_{crit} also scales with the difference in moduli, presuming again that the material from where the dislocation originates has the lower modulus.

More recent work by Anderson and Xin [7] made use of numerical simulation and presented a relationship between τ_{crit} and the moduli mismatch that includes the unstable stacking fault energy, γ_{us}, given by:

$$\tau_{crit} \approx \frac{G_2 - G_1}{G_2 + G_1}\frac{\gamma_{us}}{Gb/2\pi^2}. \quad (5)$$

In this case, the Burgers vector value b and unstable stacking fault energy γ_{us}, apply to both the donor and recipient crystals.

A distinctly different concept relates τ_{crit} to the energy penalty incurred by the residual dislocation that remains in the interface after dislocation transmission by equating the energy penalty for forming a residual dislocation with the work done by the dislocation to traverse the interface region [56, 59, 66, 78]. The length of the Burgers vector of the residual dislocation b_r scales with the lattice mismatch at the interface and its self-energy can be expressed approximately as

$$E_r \approx G|b_r|^2 \approx \tau_{crit}(w) \quad (6)$$

where G is the shear modulus of either material or can be an effective modulus value. Since the value of the b_r is the same whether the dislocation transmits from material 1 to 2 or vice versa, the effect on τ_{crit} would not be path dependent. This result is distinct

from the coherency strains created by the lattice misfit at the interface, which would create equal and oppositely signed coherency strains and hence change the attractive/repulsive nature of the interface with the impinging dislocation.

Atomistic simulations addressing slip transfer

To contrast with continuum-scale modeling, at the other end of the length-scale spectrum are atomistic models. Over the years, atomistic models have been used to capture effects at smaller length scales that more accurately describe the complexities and interplay between various phenomena during slip transfer. Atomic-scale simulations are known for their ability to account for atomic based processes that can occur within the interface, which include spreading of the absorbed dislocation, rearrangement of the atomic interface configuration, and sliding of the interface prior to impingement. Advantageously, many important material aspects, such as elastic anisotropy and dislocation dissociation, are automatically taken into account in the mechanical calculation. The mechanisms that take place at such fine atomic scales are undoubtedly valuable; however, it is well known that temperature and strain rate effects, characteristic of laboratory conditions (e.g., 77–423 K and 10^{-3}–10^{3}/s), are not well represented in such simulations.

There have been many notable works investigating slip transfer in systems such as Cu–Nb, Cu–Ag, Cu–Ni, and Ni–Al among others using atomistic methods. In atomistic simulations, perfect dislocations will dissociate into Shockley partial dislocations during glide as they approach the biphase interface in fcc metals. Typically, the partial dislocations will enter the interface region one at a time, which is a different mechanism than what is modeled in continuum models and mesoscale models. Hence, many atomistic studies have focused on and carefully analyzed the transmission of a single dislocation, and in particular, the local disruption of the interface atomic structure after a single transmission event due to the residual dislocation that is left behind [90, 91]. Besides affecting the interface structure, the presence of a residual dislocation in the interface has also been shown to hinder subsequent slip transmission events due to interactions with the next oncoming glide dislocation [33]. In addition, many atomistic studies have aimed to elucidate the relationship between the slip transfer mechanism and either Koehler image forces (forces present due to the elastic moduli mismatch across the interface), or coherency stresses (coherent interfaces) or misfit dislocations (semi-coherent and incoherent interfaces) in both bilayers and multilayered materials. Such work is much more relevant, and perhaps even necessary, for multiscale modeling activities on the mesoscale and above. In early works [25, 53], atomistic stress tensor calculations were used to show that altering the elastic constants of the individual lamellae resulted in changes in the Koehler/image barrier. More recently, Rao and Hazzledine [77] studied the effects of both Koehler stresses, which are stresses required for a dislocation to transmit against its own elastic image to cross an interface, and coherency stresses on barrier strength for oncoming dislocations in Cu–Ni bilayers and multilayers. As one may expect, the Koehler stress was found to be an effective barrier to dislocation glide. More interestingly, this work also showed that the Koehler stresses were essentially independent of the character of the oncoming glide dislocation. In short, this means that ledge formation in the interface region (occurring in the case of edge dislocation transmission but not screw dislocation transmission) is not a significant barrier for slip transmission [77]. This study also highlighted that coherency stresses impact the barrier strength of a bimetal interface in two ways: (1) coherency stresses can impart Escaig stresses (non-gliding stresses experienced by the dislocation that can alter the dislocation core size) on incoming dislocations perturbing their core structure (and the amount of perturbation can depend on the interface orientation), and (2) coherency stresses can change the Koehler stress by altering the elastic constants in the interface. In the case of a Cu–Ni transmission pathway, the latter effect of coherency stresses was shown to notably increase the Koehler stress [77]. The former effect supported earlier studies by Duesbery [23] and Escaig [27], who also showed that coherency stresses could alter the size and structure of the dislocation core resulting in a change in their core energy.

These ideas have also been extended from bilayer to multilayer systems. Experimental evidence [65, 68, 86] shows a tendency for τ_{crit} to plateau or even drop when layer thicknesses decreased below 10 nm in multilayers. Using an image model, Kamat

et al. [43] explained the decrease in τ_{crit} as a result of the interactions of the gliding dislocation with more than one interface. Approximately, image forces from three interfaces produced a result that matched values reported in literature. However, other atomistic work, such as Rao and Hazzledine [77], have argued that overlapping image forces contribute very little to the decrease in τ_{crit} and instead, attribute the cause to spreading of dislocation cores into neighboring layers.

Moving to perhaps more complex interface structures, Dikken et al. [22] recently studied a semi-coherent interface in a Ni–Al system. This system has a relatively large lattice mismatch (13%), and hence, frequent misfit dislocations are present in the interface region. This study investigated several potential pathways, including both the forward and reverse pathways (i.e., Ni–Al and Al–Ni), and whether a dislocation impinges on the interface where a misfit dislocation is located or in between them where there is perfect fcc crystallography. This work shows that the gliding dislocation is absorbed when it intersects the interface where a misfit dislocation is present, and does not get absorbed when the dislocation intersects the interface between the misfit dislocations due to augmentation in the stress state. A similar study was completed by Martinez et al. [61] in Cu–Nb. Simulations showed that if the approaching dislocation and misfit dislocation are of opposite sign and attractive, the impinging dislocation will be absorbed into the interface. Conversely, if the gliding dislocation interacts with a misfit dislocation that is of like sign, the dislocations will repel making absorption and transmission difficult.

Finally, we mention work in which changes in the propensity of slip transmission as plastic deformation developed were studied by Zhang et al. [103]. They found that transmission can become increasingly more difficult with strain for many reasons, such as: accumulated changes in interface structure, back-stresses caused by dislocations stored in the interface, and changes in interface character due to crystal reorientation during deformation. MD simulations of deformed microstructures containing both grain boundaries and biphase interfaces found that slip transfer occurs across interfaces only after considerable deformation has taken place [38].

Mesoscale mechanics simulations of slip transfer

A few modeling techniques have been introduced to treat dislocation-based phenomena at an intermediate time and length-scale regime, called the mesoscale. At this scale, plasticity is realized as a collection of individual dislocations, closely interacting with each other and internal material boundaries, such as free surfaces, grain boundaries and heterophase interfaces. Examples are discrete dislocation dynamics (DDD) [9, 16, 28, 48, 92, 96, 97] and phase field (PF) based methods [36, 45, 54, 55, 58, 83, 95], such as atomistic phase field microelasticity (APFM) [63, 64], phase field dislocation dynamics (PFDD) [11, 17], and phase field model of dislocations (PFMD) [79]. In these techniques, interactions between dislocations are based on continuum linear elastic dislocation theory. Hence, atomic motions and interactions are not explicitly calculated and much larger crystal sizes and longer timescales (on the order of seconds) can be assessed. In addition, the crystallography of slip and the type of slip systems operating are provided as input and not predicted as in atomic-scale calculations. In DDD, dislocation motion is determined by a balance of forces on nodes that lie on the dislocation line. In the PF-based techniques, the motion and configuration of individual dislocations are found by minimizing the total system energy at every strain or time increment.

It is also worth mentioning that in the category of mesoscale techniques, a few groups have used crystal plasticity based modeling to study slip transfer across grain boundaries [1, 8, 20, 26, 56, 59, 89] and bimetal interfaces [62]. For the interface, these models have adopted specialized elements at the interface or rules for slip transmission based on the LRB criteria. Although there is less activity in this type of modeling for biphase interfaces, they bear a distinct advantage of accounting for the change in interface character during deformation due to the lattice reorientation of the adjoining crystals. These models can capture the coupling between interface-affected dislocation slip in the adjoining crystals and the effect of slip on the evolution of interface character during deformation. The effect that this coupling has during deformation on the alignment of slip across an interface has been simulated in a few recent works for the Cu–Nb interface [12, 18].

A few atomically informed mesoscale micromechanical models have also been employed to study slip transmission across a bimetal interface [4–6, 33, 35, 82, 85]. For instance, Peierls–Nabarro (PN)-based models have been advanced to study screw dislocation transmission through both sliding and bonded coherent or semi-coherent interfaces in fcc bicrystals [5, 6, 84, 85]. Interface slipping was found to hinder dislocation transmission relative to the case when slipping within the interface is not allowed [6, 84]. It was further shown by Shehadeh et al. [82], who used *ab initio* methods to calculate generalized stacking fault energy (GSFE) curves to describe dislocation dissociation in both Cu and Ni, that allowing the impinging dislocations to dissociate lowers the critical stress for transmission.

DDD models have been applied to grain boundaries in single-phase materials. Many excellent developments in both dislocation reactions, hardening mechanisms like latent hardening, dislocation substructure formation, and behavior of high-velocity dislocations have been made with DDD codes [9, 16, 28, 48, 92, 96, 97]. Less work, however, has treated the interaction of dislocations with biphase interfaces. A few notable examples are applications to multilayers with impenetrable boundaries [2, 3, 29, 31]. The focus of these works has been on modeling confined layer slip (CLS), in which dislocations gliding on crystallographic slip planes in the layer must thread in between two neighboring, closely spaced interfaces. CLS is a slip mechanism proposed to operate in fine NL composites, particularly as the spacing reduces below 100 nm [67]. In the DDD models, the interface was comprised of pre-deposited dislocations or misfit dislocations and interactions between these interfacial dislocations and threading ones were found to be the key strengthening mechanism. When the layers become too fine, say 10 nm or below, CLS is assumed not to predominate and slip transmission prevails in determining strength. Later DDD models by Zbib and coworkers [101] have been developed to consider interfaces that are penetrable or shearable and used to relate atomic structure (coherency vs incoherency) with the response to intersecting gliding dislocations.

In recent years, investigations of dislocation interactions, motion, and structure using phase field methods have increased in number. In this arena, however, there have been only a few studies addressing interfaces (particularly biphase interfaces) [58] and slip transmission through these interfaces [102, 105]. Louchez et al. [58] investigated fcc/hcp interfaces that formed via the glide of partial dislocations. Zheng et al. [105] modeled slip transmission events across Ni–Ni interfaces, allowing for the impinging dislocations to be extended into partials and the interface to slide. However, since the material was the same on both sides of the interface, differences in elastic moduli and lattice parameters between two metals and any residual dislocations formed in the interface after transmission would not need to be taken into account. Last, Zeng et al. [102] made an attempt at considering slip transmission of perfect dislocations across several bimetal systems. Their formulation included several aspects of bimetal interfaces in the phase field model, including Koehler forces, coherency stresses, and residual dislocations in the interface. Furthermore, the study described by Zeng et al. addresses both edge and screw transmission in five fcc/fcc material systems. To the authors' knowledge, this is the broadest study of slip transfer in bimaterial systems at the mesoscale. For this reason, we have chosen to summarize this model in some detail in the next section. We will also use the results presented in this article as a benchmark for comparison with other results available in the literature later in the "The critical transmission stress" section.

Phase field dislocation dynamics (PFDD)

In this section we briefly review the PFDD formulation for a bimetal interface, first presented in [102]. We then discuss results for several fcc/fcc systems and compare the trends to guidelines provided by continuum models and calculations from other mesoscale methods. The system of interest is comprised of two fcc materials joined at a single interface. The two crystals have a cube-on-cube orientation relationship and are joined at their mutual (001) plane, which defines the interface normal.

PFDD bimetal interface formulation

In the PFDD methodology, evolution of the system variables is dictated by minimizing the total energy of the system. In the case of a bimaterial system, the total energy has three key terms: the elastic strain energy, E^{strain}, the core energy, E^{core}, and the energy

required to form a residual dislocation in the interface region following a slip transmission event, E^{res}, which is explicitly expressed as:

$$E(\zeta, \epsilon_{ij}^{v}) = E^{\text{strain}}(\zeta, \epsilon^{v}) + E^{\text{core}}(\zeta) + E^{\text{res}}(\zeta)\,. \tag{7}$$

Each energy term in Eq. 7 is a function of the order parameters or phase field variables, ζ. The order parameters are scalar-valued, and they track the location of the dislocation and the regions that have been slipped. In the case of PFDD, each order parameter is associated with a perfect dislocation slip system (although this is not the case of all phase field approaches directed toward modeling dislocation dynamics, see [64]). Hence, nonzero, integer values of an order parameter indicate regions that have been slipped by one or more perfect dislocations associated with that order parameter (through slip direction and slip plane normal). The order parameters can have both positive and negative values, distinguishing between positive and negative dislocations. Regions, where the order parameter transitions between integer values (e.g., 0–1, or 1–2), indicate where the dislocation line itself is. The order parameters are not restricted to only integer values, and can represent fractional amounts of dislocation. Linear combinations of multiple active order parameters on a single slip plane can produce and represent partial dislocations. In the case of fcc metals, 12 active order parameters are needed to fully describe dislocation activity in a crystal.

The strain energy E^{strain} is a function of the plastic strain ϵ_{ij}^{p} and an eigenstrain ϵ_{ij}^{v} since this system contains an inhomogeneity. The motion and interaction of dislocations in the crystal control the plastic strain, ϵ_{ij}^{p}, and thus, ϵ_{ij}^{p} can be expressed as a direct function of the active phase field variables, as follows [45]:

$$\epsilon_{ij}^{\text{p}}(\mathbf{x}, t) = \frac{1}{2}\sum_{\alpha=1}^{N} \zeta^{\alpha}(\mathbf{x}, t)\delta_{\alpha}\left(s_i^{\alpha} m_j^{\alpha} + s_j^{\alpha} m_i^{\alpha}\right), \tag{8}$$

where N is the number of slip systems, $\mathbf{s}^{\alpha}$ is the direction of the Burgers vector, $\mathbf{m}^{\alpha}$ is the slip plane normal, and δ_{α} is a Dirac distribution supported on slip plane α.

The virtual or eigenstrain, ϵ_{ij}^{v} is calculated with the viewpoint that one material in the bimetal system is the matrix (material 1) and the other an inhomogeneity (material 2) bearing different elastic moduli. The image stresses (or Koehler forces) due to the differences in the elastic moduli between the two materials are modeled using the Eshelby inclusion method [69]. Using this concept, the strain, ϵ_{ij}^{0} is introduced as:

$$\epsilon_{ij}^{0}(\mathbf{x}) = \begin{cases} \epsilon_{ij}^{p}(\mathbf{x}) & \text{if} \quad \mathbf{x} \in \text{ material 1} \\ \epsilon_{ij}^{p}(\mathbf{x}) + \epsilon_{ij}^{v}(\mathbf{x}) & \text{if} \quad \mathbf{x} \in \text{ material 2.} \end{cases} \tag{9}$$

Using stress equilibrium and the principle of superposition provides the following expression for the total strain $\epsilon_{ij}(\mathbf{x})$ [52]:

$$\begin{aligned} \epsilon_{ij}(\mathbf{x}) = & \overline{\epsilon_{ij}^{0}} + \fint \hat{G}_{jk}(\mathbf{k}) k_i k_l C_{klmn}^{(1)} \hat{\epsilon}_{mn}^{0}(\mathbf{k}) e^{ikx} \frac{d^3k}{(2\pi)^3} \\ & + S_{ijkl}^{(1)} \sigma_{kl}^{app} + \epsilon_{ij}^{mis}(\mathbf{x}). \end{aligned} \tag{10}$$

where the superscript $\hat{}$ stands for the Fourier transformation, $G_{ki}(\mathbf{x})$ is the elastic Green's function, k_i is the wave number vector, $\fint$ represents the principal value of the integral, $\overline{\epsilon_{ij}^{0}} = \frac{1}{V}\int \epsilon_{ij}^{0}(\mathbf{x}) d^3\mathbf{x}$ is the average stress-free strain and V is the volume of the computational domain, $S_{ijkl}^{(1)}$ is the compliance tensor in material 1, and σ_{ij}^{app} is the externally applied stress.

We also define $C_{ijkl}^{(1)}$ and $C_{ijkl}^{(2)}$ as the stiffness tensors in materials 1 and 2, respectively, $\Delta S_{mnpq}(\mathbf{x}) = \left(C_{mnpq}(\mathbf{x}) - C_{mnpq}^{(1)}\right)^{-1}$ is only defined in material 2, and $C_{mnpq}(\mathbf{x})$ is a stiffness tensor defined as:

$$C_{mnpq}(\mathbf{x}) = \begin{cases} C_{mnpq}^{(1)} & \text{if} \quad \mathbf{x} \in \text{ material 1} \\ C_{mnpq}^{(2)} & \text{if} \quad \mathbf{x} \in \text{ material 2} \end{cases} \tag{11}$$

Under the assumption of additive decomposition of strain, the misfit strain, $\epsilon_{ij}^{\text{mis}}$ can also be seen in Eq. 10. These misfit strains (or coherency strains) are present at the interface due to differences in the lattice parameters between the two materials. The material with the larger lattice parameter will be in compression, while the material with the smaller lattice parameter will have an equal and opposite tensile field. These strains preserve coherency at the interface.

Application of this formulation is restricted to the study to coherent interfaces or semi-coherent interfaces where the misfit dislocation is spread apart with large regions of coherent interface in between them. This assumption corresponds to systems with a lattice mismatch of 3.5% or less. In this case the misfit strains are calculated by assuming plane stress within

the local interface coordinate system and then transforming the strain tensor into the global coordinate system. In principle, however, the expression in Eq. 10 need not be limited to coherent interfaces. For instance, the misfit strains can be informed using experiment or atomistic simulations [102], or calculated with different analytical methods.

Using Eqs. 10 and 9, the elastic strain energy can be defined as [102]:

$$\begin{aligned} E^{\text{strain}} &= E^{eq} + \Delta E = \frac{1}{2}\int \hat{A}_{mnuv}(\mathbf{k})\left(\hat{\epsilon}^{\text{v}}_{mn}(\mathbf{k}) \right. \\ &\left. + \hat{\epsilon}^{\text{p}}_{mn}(\mathbf{k})\right)\left(\hat{\epsilon}^{v*}_{uv}(\mathbf{k}) + \hat{\epsilon}^{p*}_{uv}(\mathbf{k})\right)\frac{d^3k}{(2\pi)^3} \\ &- \frac{1}{2}\int C^{(1)}_{ijkl}\epsilon^{\text{mis}}_{ij}(\mathbf{x})\epsilon^{\text{mis}}_{kl}(\mathbf{x})d^3\mathbf{x} \\ &- C^{(1)}_{ijkl}\int \left(\epsilon^{\text{v}}_{ij}(\mathbf{x}) + \epsilon^{\text{p}}_{ij}(\mathbf{x})\right)\epsilon^{\text{mis}}_{kl}(\mathbf{x})d^3\mathbf{x} \\ &+ \int S^{(1)}_{ijkl}\sigma^{app}_{ij}C^{(1)}_{mnkl}\epsilon^{\text{mis}}_{mn}(\mathbf{x})d^3\mathbf{x} - \frac{V}{2}S^{(1)}_{ijkl}\sigma^{app}_{ij}\sigma^{app}_{kl} \\ &- \sigma^{app}_{ij}\int \left(\epsilon^{\text{v}}_{ij}(\mathbf{x}) + \epsilon^{\text{p}}_{ij}(\mathbf{x})\right)d^3x \\ &- \frac{1}{2}\int_2 \left(C^{(1)}_{ijmn}\Delta S_{mnpq}(\mathbf{x})C^{(1)}_{pqkl} + C^{(1)}_{ijkl}\right)\epsilon^{\text{v}}_{ij}(\mathbf{x})\epsilon^{\text{v}}_{kl}(\mathbf{x})d^3x. \end{aligned} \tag{12}$$

where $\hat{A}_{mnuv}(\mathbf{k}) = C^{(1)}_{mnuv} - C^{(1)}_{kluv}C^{(1)}_{ijmn}\hat{G}_{ki}(\mathbf{k})k_jk_l$. The first integral describes the internal strain energy due to elastic interactions between the plastic and virtual strains. The second, third, and fourth terms describe the internal strain energy due to the presence of misfit strains at the interface including interactions between the misfit strains with the plastic and virtual strains, and also the applied stress. Like the fourth term, the fifth and sixth terms also depend on the externally applied stress and describe interactions with the plastic and virtual strains, and any additional internal strain energy. The final integral accounts for elastic strain energy due to the presence of the inhomogeneity, which generates an internal stress state due to the difference in elastic moduli between the two bicrystals.

The energy term E^{core} represents the energy expended as a single dislocation glides through the crystal lattice by breaking and reforming atomic bonds. In other words, there is some increase in energy, which is often referred to as the Peierls potential, associated with moving the dislocation through the crystal lattice. Consequently, the core energy term is nonzero in regimes where the phase field variables are nonzero, non-integer values (e.g., when it changes from 0 to 1), which also represent the location of dislocation lines. In contrast, when the order parameters are (nonzero) integer values, the dislocation(s) have already traversed the slip plane leaving restored crystallography behind and the core energy term is zero.

As in prior works [46, 52, 95], this energy barrier is represented with a sinusoidal function. A sinusoidal function conveniently exhibits a periodicity that follows the regular atomic lattice of a cubic crystal structure. This model resembles the shape of the change in energy with global displacement of half the crystal with respect to the other half on the {111} plane in the $<110>$ direction. Its general form follows well that predicted by DFT and MD [39–42]. It corresponds to the local shift a perfect dislocation causes as it glides on the {111} plane in the $<111>$ direction. This approximation is best applied to perfect dislocations, but should be replaced by a full 2D γ-surface in the event that partials are modeled [42]. Furthermore, because this term accounts for nonlinear effects near the dislocation core region, it is only dependent on the active phase field variables and has no dependency on the virtual strains. The expression for E^{core} is then given by:

$$E^{\text{core}} = \sum_{\alpha=1}^{N}\int B\sin^2(\pi\zeta^{\alpha}(\mathbf{x}))\delta_{\alpha}\mathrm{d}^3x\,, \tag{13}$$

where B defines the magnitude of the energy barrier. This magnitude can be informed or calculated in various ways including through the use of atomistic methods. In this work, we have chosen to use a model from [73], which relates B to the properties of the material as follows:

$$B = \left(\frac{1}{2\pi}\right)^2\frac{1}{d}C'_{ijkl}b_ib_km_jm_l, \tag{14}$$

where $\mathbf{b}$ is Burgers vector, $\mathbf{m}$ is slip plane normal and C'_{ijkl} is the stiffness tensor in the local coordinate system of the slip system of the active phase field variable. In the PFDD results, presented in the following sections, elastic isotropy is assumed; hence, C'_{ijkl} bears no directional dependence and equals the stiffness tensor in the global coordinate system, C_{ijkl}. It is noted that because of the material dependence of B through the stiffness tensor, the values of E^{core} will depend on whether the dislocation is moving in material 1 or material 2.

The final energy term needed to calculate the total system energy shown in Eq. 7 is the energy required to form a residual dislocation in the interface following a slip transmission event, E^{res}. A residual dislocation remains in the interface due to the different Burgers vectors in each material. Once a dislocation transmits into the recipient material, a fractional dislocation will remain to accommodate the change in Burgers vector that the dislocation has undergone. Hence, E^{res} is nonzero only in the event that a dislocation transmits from material 1 to material 2 across the interface. Therefore, E^{res} is only dependent upon the phase field variables and not the virtual strains, similar to the core energy in Eq. 13.

In the PFDD model, the interface is comprised of two planes, one donated by material 1 and the other from material 2. Within this interface region, the presence of the residual dislocation will cause a net displacement, $\mathbf{u}_r = \zeta^{(2)}\mathbf{b}^{(2)} - \zeta^{(1)}\mathbf{b}^{(1)}$, where the notation $\zeta^{(1,2)}$ indicates the value of the order parameter on the interface plane contributed by material 1 and 2, respectively. Consequently, the displacement $\mathbf{u}_r$ will give rise to distortions, $\beta_{ij}^{(1,2)}$, on either side of the interface. These distortions can be expressed in terms of the order parameter similar to the plastic strain shown in Eq. 8

$$\beta_{ij}^{(1,2)} = \zeta^{(1,2)} s_i^{(1,2)} m_j^{(1,2)}, \tag{15}$$

where once again it is noted that $\zeta^{(1,2)}$ indicates the value of the order parameter on the interface plane contributed by material 1 and 2, respectively. As before, **s** and **m** are the slip direction and slip plane normal. These distortions can be related to a stress tensor using Hooke's Law, $\sigma_{ij}^{(1,2)} = C_{ijkl}^{*(1,2)} \cdot \epsilon_{kl}^{(1,2)}$, where $\epsilon_{kl}^{(1,2)}$ is the symmetric part of $\beta_{ij}^{(1,2)}$. In expressing $\sigma_{ij}^{(1,2)}$ using Hooke's Law, the assumption is made that these quantities are related through a nonlinear modulus for the interface $C_{ijkl}^{*(1,2)}$. Unfortunately, values for $C_{ijkl}^{*(1,2)}$ are not generally known for interfaces. In light of this, $C_{ijkl}^{*(1,2)}$ is chosen to be the elastic moduli of the donor material ($C_{ijkl}^{(1)}$) on the interface plane contributed by material 1 and, likewise, the moduli of the recipient material ($C_{ijkl}^{(2)}$) on the interface plane contributed by material 2. The tractions on either side of the interface due to the presence of a residual dislocation can then be determined as

$$\tau_i^{(1,2)} = \sigma_{ij}^{(1,2)} \cdot n_j, \tag{16}$$

where **n** is the interface normal. Finally, the energy associated with formation of the residual is given by [102]:

$$E^{\text{res}} = \int_S \left| \boldsymbol{\tau}^{(1)} \cdot \mathbf{u}_r^{(1)} - \boldsymbol{\tau}^{(2)} \cdot \mathbf{u}_r^{(2)} \right| \mathrm{d}S. \tag{17}$$

With the total system energy formulated, the key parameters in the model, namely the phase field variables and the virtual strain tensor, can be calculated as they evolve in time. Here, the evolution of the phase field variables and virtual strains is determined by minimization of the total system energy in Eq. 7. As in prior work [45, 52, 95, 102], minimization is carried out using the following set of time-dependent Ginzburg-Landau (TDGL) kinetic equations [30, 49]:

$$\begin{aligned} \frac{\partial \zeta^{\alpha}(\mathbf{x},t)}{\partial t} &= -L \frac{\delta E(\zeta, \epsilon^{\text{v}})}{\delta \zeta^{\alpha}(\mathbf{x},t)} \quad \text{in materials 1 and 2,} \\ \frac{\partial \epsilon_{ij}^{v}(\mathbf{x},t)}{\partial t} &= -K \frac{\delta E(\zeta, \epsilon^{\text{v}})}{\delta \epsilon_{ij}^{\text{v}}(\mathbf{x},t)} \quad \text{in material 2 ,} \end{aligned} \tag{18}$$

where L is a kinetic coefficient that defines the timescale of the simulation, and K is a material constant related to material 2. Although Eq. 18 shows the time-dependent form of the GL kinetic equations, in results discussed in subsequent sections the system is evolved to an equilibrium state; that is, when the left-hand sides of Eq. 18 become zero. Consequently, the equilibrium state is independent of parameters L and K and the results best apply to quasi-static loading conditions. Equation 18 shows that through the total system energy these two TDGL equations are coupled and must be evolved together. This coupling is most obvious in the case where a dislocation in moving within the inhomogeneous region (i.e., material 2). Solution of the coupled TDGL equations is achieved through a nested iterative loop scheme, which first explicitly evolves the virtual strains in the system, followed by an explicit evolution of the order parameters (or dislocation network). The iteration over the order parameters is sub-cycled until convergence is achieved, before the virtual strains are evolved again. In all cases convergence is achieved when the change in the total system energy is less

than 10^{-7}. We also note that the virtual strains only need to be evolved in material 2 (where the inhomogeneity exists), while the order parameters are evolved in both material 1 and 2. In material 1, the virtual strains are zero since this is considered the matrix material.

The critical transmission stress

In this section the application of the bicrystal PFDD model to study the energetics of slip transmission across biphase interfaces is reviewed. Of the fcc/fcc bimetal systems with relatively low lattice mismatch, Cu–Ni is on of the most commonly modeled systems. Hence, the example of a Cu–Ni bicrystal is first presented to discuss some interesting details in path dependence and also for initial comparison with critical transmission stress values calculated with other mesoscale approaches available in the literature. Some additional calculations for a broad range of systems to elucidate material effects then follow.

The Cu–Ni bicrystal system

In this first example problem, the Cu and Ni fcc crystals are joined at a mutual (001) plane, which forms the interface between the two materials. Both crystals exhibit cubic elastic anisotropy and the corresponding stiffness tensor C_{ijkl} could be incorporated in a straightforward manner in the PFDD calculation. However, to ease in computation and to enable direct comparisons with the guidelines presented previously in the "Guidelines for slip transfer" section, elastic isotropy is assumed. Qualitatively the trends will be the same but quantitatively, the elastic energies will be in error by 20–30% [34, 87, 88]. Cu and Ni also differ in lattice parameters by about 2.5%, which will generate nonzero misfit strains at the coherent interface. All simulations were completed in a computational cell with periodic boundary conditions and a size of $64a_{(1,2)} \times 2a_{(1,2)} \times 64a_{(1,2)}$ where a is the lattice parameter of material 1 or material 2 when appropriate. Due to the periodic boundary conditions, image stresses from neighboring cells must be considered. For the case of dislocation transmission across a bimetal interface, we are focused only on a local interface region, particularly where the coherency stresses and formation of a residual dislocation can impact the transmission process. In this case, the simulation cell size of $64a_{(1,2)} \times 2a_{(1,2)} \times 64a_{(1,2)}$ is sufficient so that the presence of image dislocations in neighboring periodic cells do not affect the dislocation motion or the calculation of the critical transmission stress. In addition, the interface inside the computational cell was the only one considered for modeling slip transmission events. Additional interfaces between materials present at the computational cell boundaries were considered as impenetrable.

Simulations were completed to determine the critical transmission stress, τ_{crit}, required for the slip transmission of both an edge and screw perfect dislocation. For these simulations, the initial (either edge or screw) dislocation was placed in the donor material (material 1) and driven toward the interface with an applied shear stress. Figure 2a presents the simulation configuration for edge dislocation transmission with a Burgers vector of $[\bar{1}10]$ and a line direction of $[11\bar{2}]$. Similarly, Fig. 2b shows the configuration for slip transmission of a perfect screw dislocation with a Burgers vector and line direction of $[1\bar{1}0]$. We note that in the case of edge dislocation transmission there is an additional rotation of the interface (shown in Fig. 2a) with respect to the dislocation line direction due to the fcc crystal structure that is not present in the screw dislocation configuration. Rather in the screw dislocation case, the line direction is parallel to the interface. Once the dislocation impinged on the interface, the applied shear stress was incrementally increased until the dislocation fully pushed through the interface exiting into material 2. The applied stress at this point of transmission resolved onto the slip plane of the gliding dislocation defines the critical transmission stress, τ_{crit}. In other words, the critical transmission stress corresponds to the resolved shear stress on the slip system when the applied stress just reaches a level that allows the dislocation to push through the interface. In addition, simulations were performed for two pathways for slip transmission: (1) the dislocation initially glides in Cu and transmits through the interface into Ni, and (2) the reverse pathway where the dislocation initially glides in Ni and transmits into the Cu layer. For these cases the following critical transmission stresses where calculated for edge dislocation slip transmission: $\tau_{crit} = 2.58$ GPa (Cu–Ni) and $\tau_{crit} = 5.36$ GPa (Ni–Cu) [102]. Similarly in the case of screw dislocation slip transmission:

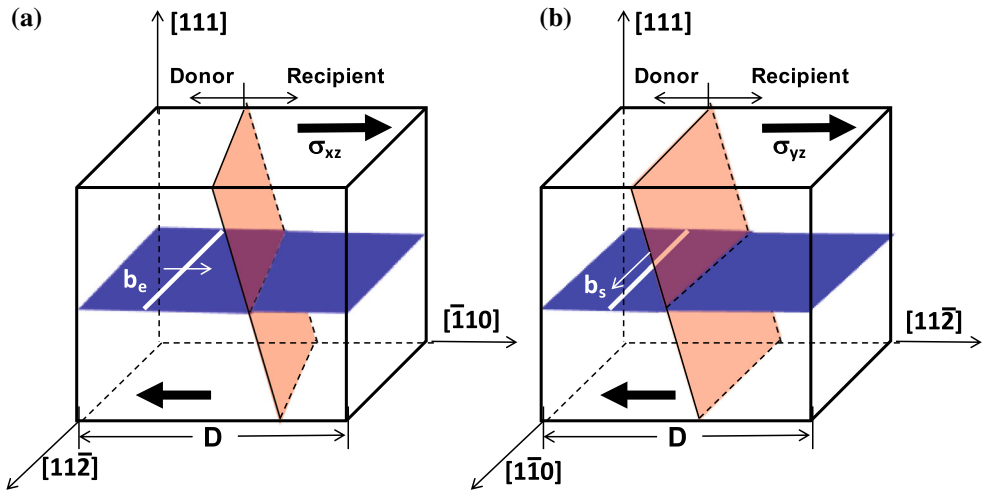

Figure 2 Schematic representation of the initial PFDD simulation setup for transmission of a perfect **a** edge dislocation and **b** screw dislocation through a bimaterial interface. A shear stress is applied that drives the dislocation toward a [001] interface. Once the dislocation impinges on the interface the applied stress is incrementally increased until the dislocation transmits through the interface. Figure taken with permission from [102].

$\tau_{crit} = 2.22$ GPa (Cu–Ni) and $\tau_{crit} = 4.69$ GPa (Ni–Cu) [102].

The first point to note from the calculated critical transmission stress values is the pronounced asymmetry in the values between the forward and reverse transmission pathways (e.g., Cu–Ni and Ni–Cu). This asymmetry is seen in both the edge and screw transmission simulations. The resistance to slip transmission is larger when slip attempts to transmit into a recipient material with a lower shear modulus and a larger lattice parameter.

A second feature, seen in the Cu–Ni critical transmission stress results, is that for all pathways, transmission of a screw dislocation is slightly easier than transmission of an edge dislocation. This is likely due to the lower self-energy of the screw dislocation in comparison to an edge dislocation [34]. The residual dislocation left in the interface region following a screw dislocation transmission event will also be of screw type and, hence, have a lower self-energy than a residual dislocation left from an edge dislocation transmission, which will be of edge type. Transmission of a screw dislocation could be slightly easier than that of an edge dislocation as shown in the Cu–Ni data due to this difference in self-energy.

As mentioned, we can compare these values to those determined using the guidelines presented previously in the "Guidelines for slip transfer" section. For this comparison, we use isotropic, effective shear moduli for Cu and Ni, which are $G_{Cu} = 23.5$ GPa and $G_{Ni} = 49.6$ GPa, respectively. A complete comparison is not possible since many prior studies consider only the case in which a screw dislocation is moving from a donor material with a lower shear modulus to a recipient material with a higher shear modulus, which is true for the Cu–Ni transmission pathway. Using Eq. 3, we calculate $\tau_{crit} \approx 2.1396$ GPa. In contrast, using Eq. 4, we calculate $\tau_{crit} \approx 0.2391$ GPa for an interface of width $w = 20b$. This is significantly lower than the value calculated with Eq. 3. The PFDD value is actually quite close with a value $\tau_{crit} = 2.22$ GPa to that using Eq. 3. Both PFDD and Eq. 3 assume a sharp interface rather than a diffuse interface as Krzanowski did. One would expect that τ_{crit} would decrease with increasing interface diffusivity. This was also noted by Anderson et al. [6], who did a similar exercise for the Cu–Ni material system but with slightly different (larger) moduli values than those used here.

Anderson et al. [6, 85] also studied the effect of interface slip using a Peierls approach and atomic-scale calculations using Embedded Atom Model (EAM) potentials. This work particularly focused on the Cu–Ni material system with ratio of the shear moduli, G_2/G_1, having values of 1.1, 1.25 and 1.8 [85]. For the Cu–Ni system analyzed with PFDD, $G_{Ni}/G_{Cu} \approx 2.11$, which is notably larger than the values studied by Anderson et al., but closest to 1.8 for which they report critical transmission stresses ranging from $0.032\bar{G} - 0.045\bar{G}$ depending on the

coherency stresses [85], where $\bar{G} = 0.5(G_2 + G_1)$ as is used in [6]. Calculating $\bar{G}$ with moduli values listed above and normalizing the τ_{crit} value calculated with PFDD, we get $\tau_{crit}/\bar{G} = 0.061$. This is slightly larger than the range reported by Shen and Anderson in [85], but reasonably close considering the larger shear moduli ratio.

Extending to other fcc/fcc systems

Following Cu–Ni, simulations were completed for several fcc/fcc systems with coherent boundaries (i.e., lattice mismatch of <3.5%) using PFDD. Table 1 gives the PFDD calculated critical transmission stresses for both edge and screw dislocation transmission. Again, similar to the Cu–Ni case, τ_{crit} for screw dislocation transmission is slightly less than that of edge dislocation transmission for all cases. Interestingly, all systems show a significant transmission pathway asymmetry in the critical transmission stresses. Even the Ag–Au system, which has the least amount of moduli and lattice mismatch, has some dependence of the critical transmission stresses on the pathway of transmission.

As discussed previously in the "Guidelines for slip transfer" section, it has been proposed that τ_{crit} will scale with the shear modulus when the modulus of the recipient material is larger than that of the donor material [44, 74]. This scaling seems to agree with the PFDD calculations for several fcc systems and is shown in Fig. 3.

Table 2 compares calculated τ_{crit} values from the PFDD model with those calculated using with Eqs. 3 and 4 using the same elastic moduli. As expected, the values calculated with Eq. 4 are much lower than those calculated with PFDD. As discussed in the Cu–Ni case, this is due to the assumption of a diffuse interface made by Krzanowski in Eq. 4 versus the sharp interface modeled by PFDD. The τ_{crit} values calculated with PFDD compare well to values calculated with Eq. 3, especially in systems with larger moduli mismatch.

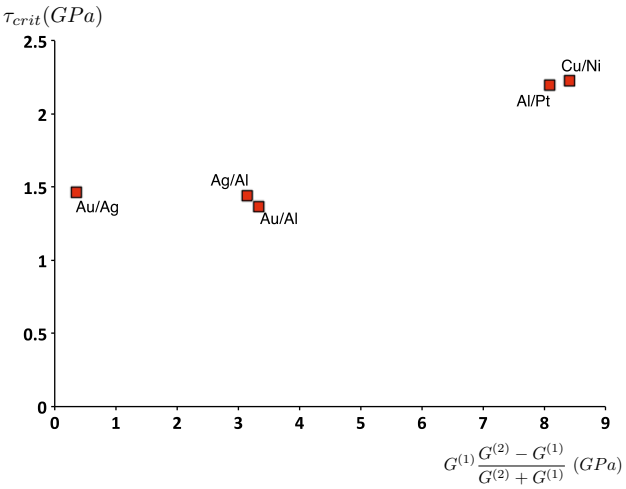

Figure 3 Critical transmission stresses for perfect screw dislocation transmission as calculated by the PFDD model and compared to the guideline proposed by Koehler and Pacheco and Mura that highlights the effect of moduli mismatch at the interface [44, 74]. Figure taken with permission from [102].

Thus far in comparing to many proposed guidelines, we have been only able to rely on a subset of our data. There are two other proposed guidelines, which allows us to also include calculations for edge dislocation transmission. The first of these is that τ_{crit} scales with the self-energy of the system. In other words, one might think that transmission will be easier if the dislocation can lower its self-energy which scales as $\sim Gb^2$. If we take Cu–Ni as an example, the transmission pathway Ni–Cu should have the lower critical transmission stress since the self-energy of a dislocation in Cu is less than that in Ni. However, Table 1 shows us this is not the case. As mentioned previously in the "Guidelines for slip

Table 1 Critical transmission stresses calculated with the PFDD model for edge and screw dislocation slip transmission in several bimaterial systems

System ($a_1 > a_2$)	Edge	Screw	System ($a_2 > a_1$)	Edge	Screw
Al/Pt	2.34	2.19	Pt/Al	5.33	4.54
Cu/Ni	2.58	2.22	Ni/Cu	5.36	4.69
Ag/Al	1.70	1.45	Al/Ag	2.48	2.20
Au/Al	1.64	1.38	Al/Au	2.55	2.20
Ag/Au	1.70	1.40	Au/Ag	2.20	1.47

The critical transmission stress is calculated as the resolved shear stress on the dislocation above which the dislocation can push through the interface. The threshold value is found by incrementing the applied stress until the dislocation can fully traverse the interface into material 2

Table 2 Critical transmission stresses (in GPa) calculated with PFDD and available continuum models (specifically those developed by: Kohler (Eq. 3), Krzanowski (Eq. 4), and Anderson et al. [6]) for transmission of a perfect screw dislocation

System	G_1	G_2	G_2/G_1	τ_{crit} PFDD [102]	τ_{crit} (Eq. 3)	τ_{crit} (Eq. 4)	$\tau_{crit}^{PFDD}/\bar{G}$ [6, 85]
Al/Pt	23.2	48.0	2.07	2.19	2.311	0.2272	0.062
Cu/Ni	23.5	49.6	2.11	2.22	2.1396	0.2391	0.061
Ag/Al	15.3	23.2	1.52	1.45	0.9073	0.0724	0.075
Au/Al	14.6	23.2	1.59	1.38	0.9566	0.0788	0.073
Au/Ag	14.6	15.3	1.05	1.47	0.0984	0.0064	0.098

In Eq. 4 an interface width of $w = 20b$ was used in all cases. Isotropic effective shear moduli values are taken from [102], and $\bar{G} = 0.5(G_2 + G_1)$. In the PFDD model, the critical transmission stress is calculated as the resolved shear stress on the dislocation above which the dislocation can push through the interface. The threshold value is found by incrementing the applied stress until the dislocation can fully traverse the interface into material 2

transfer" section, several groups [56, 59, 66, 78] have proposed that the critical transmission stress scales with the self-energy of the residual dislocation left in the interface (see Eq. 6). In Fig. 4, this is tested for the τ_{crit} associated with the easier slip transmission pathway, which would be expected to be the more likely pathway for a slip transmission event to occur. This critical transmission stress is denoted as τ_{crit}^{easy} in Fig. 4. As shown, the critical transmission stress increases with the self-energy of the residual dislocation left in the interface. It is also seen that the resistance to transmission is generally higher when lattice mismatch is higher.

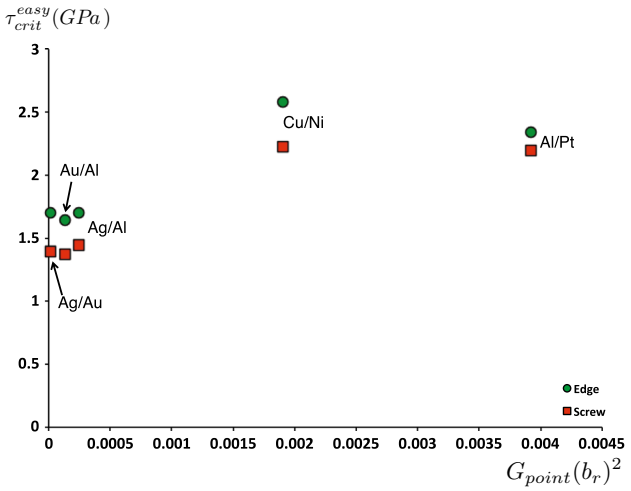

Figure 4 Critical transmission stresses for the easier transmission pathway (τ_{crit}^{easy}) for both perfect edge (green circles) and screw (red squares) dislocation transmission as calculated by the PFDD model plotted against the self-energy of the residual dislocation left in the interface following a transmission event, where b_r is the Burgers vector of the residual dislocation and G_{point} is the shear modulus of the material into which a an edge residual dislocation points to. Several works [56, 59, 66, 78] have proposed that the critical transmission stress scales with this measure. Figure taken with permission from [102].

In employing this criterion, difficultly lies in choosing the shear modulus in the interface. This shear modulus would depend on the shear moduli in the surrounding two materials and is not readily available. In Fig. 4, the shear modulus selected was that of the material into which the Burgers vector of the residual points following transmission of an edge dislocation. The results of the PFDD calculated values against this scaling are shown in Fig. 4.

Based on the energy to form a residual dislocation in the interface region, a scaling was proposed that depended on the lattice parameters and shear moduli of both the donor and recipient materials and suggested a path dependence on τ_{crit}. The scaling goes as:

$$\tau_{crit} \sim \frac{a_2 G_2}{a_1 + a_2}\left(\frac{a_1}{a_2} - \frac{G_1}{G_2}\right). \tag{19}$$

Figure 5 compares the PFDD calculated τ_{crit} values with the scaling factor in Eq. 19 for a number of bimetal systems. Overall the factor captures well the trends produced by the calculations, especially considering that it is applied the entire PFDD data set including both edge and screw dislocation transfer for both the forward and reverse transmission pathways. The consistency suggests that transmission of slip is more difficult when occurring from the material with the smaller lattice parameter to the larger one. It also indicates that slip transmission would become increasingly more difficult with increasing differences between the lattice and elastic moduli of the two materials. We also note that the scaling factor slightly under-predicts the critical transmission stress for systems with less moduli and lattice mismatch (e.g., Ag–Au, Au–Al, and Ag–Al). This may show

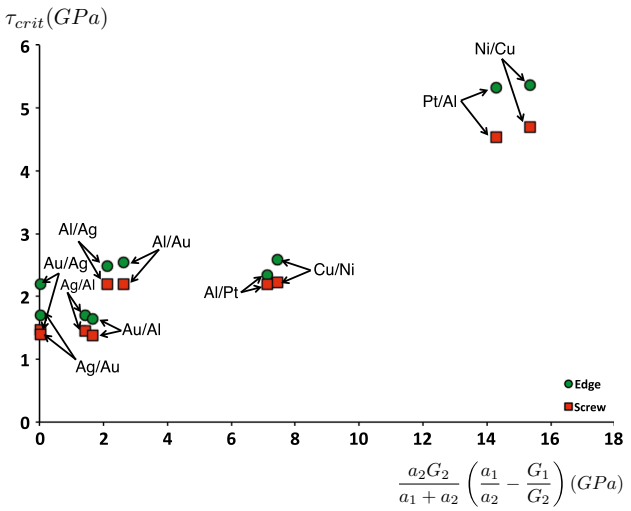

Figure 5 Calculated critical transmission stresses using the PFDD model for both perfect edge (green circles) and screw (red squares) dislocation transmission compared against the scaling guideline proposed by Zeng et al. [102]. This guideline assumes that the critical transmission stress scales with the energy required to form the residual dislocation in the interface region. Figure taken with permission from [102].

that in systems where the lattice and moduli mismatch are less significant, there are other considerations, such as core energy terms or elastic interactions, that can impact τ_{crit}. These additional terms would be accounted for in the PFDD model, but not the analytical scaling factor.

Summary and future recommendations

In this work we have summarized several mesoscale approaches that have been used to investigate and study slip transfer in heterophase interfaces. More specifically, we presented a detailed review of a PFDD model for interactions between dislocations and bimaterial interfaces that was used to calculate the energy and critical stress, τ_{crit} required to transmit a dislocation across interfaces comprised of a wide range of material combinations. These calculations involved simulations of slip transmission of a straight dislocation, of either screw or edge orientation, across interfaces created by two dissimilar crystals with an fcc crystal structure, such as Cu/Ni, Ag/Au, Al/Au, and Al/Pt, with a cube-on-cube orientation relationship. It is shown that τ_{crit} for screw oriented dislocations is lower than that for edge dislocations. Another interesting finding is an asymmetry in τ_{crit} with respect to the direction of transmission. As differences in lattice and moduli mismatch increase, the differences in τ_{crit} between the two paths, from A to B versus B to A, increase. Generally τ_{crit} is larger when the dislocation transmits from a stiffer material with a smaller lattice parameter to a softer material with a larger lattice parameter. These results were presented and discussed in terms of other values available in the literature and proposed guidelines used to determine the ease of dislocation transmission. These guidelines aim to connect τ_{crit} to material properties such as mismatch in moduli, mismatch in lattice parameters, or changes in the dislocation self-energy as it moves from one material to the other.

The demonstrations discussed here included full (or perfect) dislocations that were not extended with a stacking fault width as part of their core. In prior work, the PFDD formulation has been extended to incorporate the energetics of dislocation cores from density functional theory (DFT) calculations, enabling studies of partial dislocation formation, expansion, and deformation twinning [39–42]. The PFDD framework is capable of studying the dynamics and energetics of slip transmission of partial dislocations across biphase interfaces. Investigations into the effect of stacking fault energies on the critical thresholds for and key events involved in slip transmission would be possible. Thus far, calculations have not considered additional mechanisms that may be active in the interface plane, such as dislocation spreading in the interface. The addition of partial dislocations would be a first step in addressing such mechanisms and would enable more direct comparisons to atomistic results, which inherently take into account such dislocation dissociation reactions in fcc metals. However, even with the enhancement of the core energy in PFDD to account for partial dislocations, this term will not account for complex dislocation core behavior, such as changes in the core of the dislocation while in the interface. Rather, the expression of the core energy itself can be further developed to be more directly informed by atomistics (e.g., via a look-up table) or expanded to account for additional physics (e.g., pressure dependence of the material γ-surface). The latter case, in particular, is subject for future work.

In this article, we have focused on a particular material system, including an interface with a relatively simple crystallographic character, one that is low in energy and frequently occurring in nature. The

energetics and events involved in the slip transmission, however, would be sensitive to changes in boundary plane and orientation relationship. These degrees of freedom can alter the atomic and defect structure of the interface, and the introduction of such interface defects would affect the interactions with incoming dislocations and in particular the path dependence of τ_{crit}. In these mesoscale PFDD calculations, the asymmetry in τ_{crit} is due to lattice and moduli mismatch. Only coherent interfaces, containing no misfit dislocations, were considered. Prior atomistic works have shown that misfit dislocations can also alter the critical transmission stress τ_{crit} and the associated pathway asymmetry. An atomistic simulation study on Al–Ni by Dikken et al. [22] observed that when the dislocation moved from Al to Ni, it was absorbed into the interface. In the reverse pathway, Ni–Al, the dislocation was absorbed and then transferred into Al. The reason for the path dependence in τ_{crit} is different since PFDD cannot capture the atomic-scale processes involved in dislocation absorption. Similarly, Anderson et al. [6] studied the Al–Ni system using an atomistic approach. They reported a value of $\tau_{crit} = 0.05G_{Al}$ and also found that the presence of misfit dislocations could play a significant roll in slip prevention across interfaces.

Following these ideas, biphase interfaces between crystals of dissimilar crystal structure, such as bcc/fcc or bcc/hcp combinations, would open an entirely new set of interfaces, differing not only in defect structure but also the slip systems preferred on either side of the interface. The fundamental framework of the PFDD model introduced here can, in principle, treat these cases. Not many phase field dislocation models, however, have treated alternate crystal structures apart from fcc. One notable exception is the work by Louchez et al. [58] who model the transformation from fcc to hcp via the motion of Shockley partials. In addition, a small effort toward extension to bcc metals was outlined in [11]. Thus, fundamental future extensions of the PFDD technique would include treating crystals of alternate atomic structures. Further, the length and timescales of the phase field technique would be capable of studying the effects of two or more dislocations transmitting in sequence, accumulated residual dislocations in the interface, or pile-ups in the crystal interacting with an interface.

Acknowledgements

A. H. would like to acknowledge support from the Los Alamos National Laboratory Directed Research and Development (LDRD) Program under the Project # 20160156ER. I.J.B. acknowledges financial support from the National Science Foundation Designing Materials to Revolutionize and Engineer our Future (DMREF) Program (NSF CMMI-1729887). B. L. acknowledges financial support from the Department of Defense (DoD) through the National Defense Science & Engineering Graduate Fellowship (NDSEG) Program.

References

[1] Acharya A (2007) Jump condition for GND evolution as a constraint on slip transmission at grain boundaries. Philos Mag 87(8–9):1349–1359

[2] Akasheh F, Zbib HM, Hirth JP, Hoagland RG, Misra A (2007) Dislocation dynamics analysis of dislocation intersections in nanoscale metallic multilayered composites. J Appl Phys 101:084314

[3] Akasheh F, Zbib HM, Hirth JP, Hoagland RG, Misra A (2007) Interaction between glide dislocations and parallel interfacial dislocations in nanoscale strained layers. J Appl Phys 102:034314

[4] Anderson PM, Foecke T, Hazzledine PM (1999) Dislocation-based deformation mechanisms in metallic nanolaminates. MRS Bull 24(2):27–33

[5] Anderson PM, Li C (1995) Hall-petch relations for multilayered materials. Nanostruct Mater 5(3):349–362

[6] Anderson PM, Rao S, Cheng Y, Hazzledine PM (1999) The critical stress for transmission of a dislocation across an interface: results from peierls and embedded atom models. Mater Res Soc Symp Proc 586:267–272

[7] Anderson PM, Xin XJ (2002) The critical shear stress to transmit a peierls screw dislocation across a non-slipping interface. In: Chuang TJ, Rudnicki JW (eds) Multiscale fracture and deformation in materials and structures: James R. Rice 60th anniversary volume. Kluwer Academic Publishers, Dordrecht, p 87

[8] Ashmawi WM, Zikry MA (2002) Prediction of grain-boundary interfacial mechanisms in polycrystalline materials. J Eng Mater Technol 124(1):88–96

[9] Bertin N, Capolungo L, Beyerlein IJ (2013) Hybrid dislocation dynamics based strain hardening constitutive model. Int J Plast 49:119–144

[10] Beyerlein IJ, Demkowicz MJ, Misra A, Uberuaga BP (2015) Defect-interface interactions. Prog Mater Sci 74:125–210

[11] Beyerlein IJ, Hunter A (2016) Understanding dislocation mechanics at the mesoscale using phase field dislocation dynamics. Philos Trans R Soc A 374:20150166

[12] Beyerlein IJ, Mayeur JR (2015) Mesoscale investigations for the evolution of interfaces in plasticity. Curr Opin Solid State Mater Sci 19:203–211

[13] Beyerlein IJ, Mayeur JR, Zheng S, Mara NA, Wang J, Misra A (2014) Emergence of stable interfaces under extreme plastic deformation. Proc Natl Acad Sci 111(12):4386–4390

[14] Beyerlein IJ, Wang J, Kang K, Zheng SJ, Mara NA (2013) Twinnability of bimetal interfaces in nanostructured composites. Mater Res Lett 1(2):89–95

[15] Bieler TR, Eisenlohr P, R F, Kumar D, Mason DE, Crimp M, Raabe D (2009) The role of heterogeneous deformation on damage nucleation at grain boundaries in single phase metals. Int J Plast 25(9):1655–1683

[16] Cai W, Bulatov VV (2004) Mobility laws in dislocation dynamics simulations. Mater Sci Eng A 387–389:277–281

[17] Cao L, Hunter A, Beyerlein IJ, Koslowski M (2015) The role of partial mediated slip during quasi-static deformation of 3d nanocrystalline metals. J Mech Phys Solids 78:415–426

[18] Carpenter JS, McCabe RJ, Mayeur JR, Mara NA, Beyerlein IJ (2015) Interface-driven plasticity: the presence of an interface-affected zone in metallic lamellar composites. Adv Eng Mater 17:109–114

[19] Carpenter JS, Nizolek T, McCabe RJ, Zheng SJ, Scott JE, Vogel SC, Mara NA, Pollock TM, Beyerlein IJ (2015) The suppression of instabilities via biphase interfaces during bulk fabrication of nanograined zirconium. Mater Res Lett 3:50–57

[20] Cermelli P, G ME (2002) Geometrically necessary dislocations in viscoplastic single crystals and bicrystals undergoing small deformations. Int J Solids Struct 39(26):6281–6309

[21] Clark WAT, Wagoner RH, Shen ZY, Lee TC, Robertson IM, Birnbaum HK (1992) On the criteria for slip transmission across interfaces in polycrystals. Scr Metall Mater 26(2):203–206

[22] Dikken RJ, Khajeh Salehani M (2017) Edge dislocation impingment on interfaces between dissimilar metals. https://hal.archives-ouvertes.fr/hal-01572509. Accessed 22 Aug 2017

[23] Duesbery MS (1989) The dislocation core and plasticity. In: Nabarro FRN (ed) Dislocations in solids: basic problems and applications, vol 8. Elsevier, Amsterdam, p 67

[24] Dundurs J (1967) On the interaction of a screw dislocation with inhomogeneities. In: Eringen AC (ed) Recent advances in engineering science, vol 2. Gordon & Breach Science Publishers Ltd., Cambridge, pp 223–233

[25] Egami T, Maeda K, Vitek V (1980) Structural defects in amorphous solids a computer simulation study. Philos Mag A 41:883–901

[26] Ekh M, Bargmann S, Grymer M (2011) Influence of grain boundary conditions on modeling of size-dependence in polycrystals. Acta Mech 218(1–2):103–113

[27] Escaig B (1968) Cross-slipping process in the fcc structure. In: Rosenfield AR, Hahn GT, Bement AL Jr, Jaffee RI (eds) Proceedings of the battelle colloquium dislocation dynamics. McGraw-Hill, New York, p 655

[28] Espinosa HD, Panico M, Berbenni S, Schwarz KW (2006) Discrete dislocation dynamics simulations to interpret plasticity size and surface effects in freestanding fcc thin films. Int J Plast 22:2091–2117

[29] Ghoniem NM, Han X (2005) Dislocation motion in anisotropic multilayer materials. Philos Mag 85(24):2809–2830

[30] Ginzburg VL (1945) The dielectric properties of crystals of seignettcelectric substances and of barium titanate. Zh Eksp Teor Fiz 15:739–749

[31] Han X, Ghoniem NM (2005) Stress fields and interaction forces of dislocations in anisotropic multilayer thin films. Philos Mag 85(11):1205–1225

[32] Head AK (1953) X. The interaction of dislocations and boundaries. Lond Edinb Dublin Philos Mag J Sci 44(348):92–94

[33] Henager CH Jr, Hoagland RG (2004) A rebound mechanism for misfit dislocation creation in metallic nanolayers. Scr Mater 50(5):701–705

[34] Hirth JP, Lothe J (1968) Theory of dislocations. McGraw-Hill, New York

[35] Hoagland RG, Mitchell TE, Hirth JP, Kung H (2002) On the strengthening effects of interfaces in multilayer fcc metallic composites. Philos Mag A 82(4):643–664

[36] Hu SY, Li YL, Zheng YX, Chen LQ (2004) Effect of solutes on dislocation motion – a phase-field simulation. Int J Plast 20(3):403–425

[37] Huang H, Spaepen F (2000) Tensile testing of free-standing cu, ag and al thin films and ag/cu multilayers. Acta Mater 48(12):3261–3269

[38] Huang S, Beyerlein IJ, Zhou C (2017) Nanograin size effects on the strength of biphase nanolayered composites. Sci Rep 7(1):11251

[39] Hunter A, Beyerlein IJ (2014) Predictions of an alternative pathway for grain-boundary driven twinning. Appl Phys Lett 104(233112):1–4

[40] Hunter A, Beyerlein IJ (2014) Stacking fault emission from grain boundaries: material dependencies and grain size effects. Mater Sci Eng A 600:200–210

[41] Hunter A, Beyerlein IJ (2015) Relationship between monolayer stacking faults and twins in nanocrystals. Acta Mater 88:207–217

[42] Hunter A, Zhang RF, Beyerlein IJ (2014) The core structure of dislocation and their relationship to the material γ-surface. J Appl Phys 115:134314

[43] Kamat SV, Hirth JP, Carnahan B (1987) Image forces on screw dislocations in multilayer structures. Scr Metall Mater 21:1587–1592

[44] Koehler JS (1970) Attempt to design a strong solid. Phys Rev B 2(2):547–551

[45] Koslowski M, Cuitiño A, Ortiz M (2002) A phase-field theory of dislocations dynamics, strain hardening and hysteresis in ductile single crystals. J Mech Phys Solids 50(12):2597–2635

[46] Koslowski M, Wook Lee D, Lei L (2011) Role of grain boundary energetics on the maximum strength of nano crystalline nickel. J Mech Phys Solids 59:1427–1436

[47] Krzanowski JE (1991) The effect of composition profile shape on the strength of metallic multilayer structures. Scr Metall Mater 25(6):1465–1470

[48] Kubin L (2013) Dislocations. Mesoscale simulations and plastic flow. Oxford University Press, Oxford

[49] Landau LD (1937) On the theory of phase transitions. i Zh Eksp Teor Fiz 7:19–42

[50] Lee TC, Robertson TC, Birnbaum HK (1990) Tem in situ deformation study of the interaction of lattice dislocations with grain boundaries in metals. Philos Mag A 62(1):131–153

[51] Lee TC, Robertson TC, Birnbaum HK (1990) An in situ transmission electron microscope deformation study of the slip transfer mechanisms in metals. Metall Trans A 21(9):2437–2447

[52] Lei L, Marian JL, Koslowski M (2013) Phase-field modeling of defect nucleation and propagation in domains with material inhomogeneities. Modell Simul Mater Sci Eng 21(025009):1–15

[53] Leibfried G, Breuer N (1978) Point defects in metals, vol. 1, springer tracts in modern physics, vol 81. Springer, Berlin

[54] Levitas VI, Javanbakht M (2012) Advanced phase-field approach to dislocation evolution. Phys Rev B 14:140101

[55] Levitas VI, Javanbakht M (2015) Thermodynamically consistent phase field approach to dislocation evolution at small and large strains. J Mech Phys Solids 82:345–366

[56] Lim LC, Raj R (1985) Continuity of slip screw and mixed crystal dislocations across bicrystals of nickel at 573k. Acta Metall 33(8):1577–1583

[57] Louat N (1985) Alloys, strong at room and elevated temperatures from powder metallurgy. Acta Metall 33(1):59–69

[58] Louchez MA, Thuinet L, Besson R, Legris A (2017) Microscopic phase-field modeling of hcp|fcc interfaces. Comput Mater Sci 132:62–73

[59] Ma A, Roters F, Raabe D (2006) On the consideration of interaction between dislocations and grain boundaries in crystal plasticity finite element modeling–theory, experiments, and simulations. Acta Metall 54(8):2181–2194

[60] Mara NA, Beyerlein IJ (2014) Review: effect of bimetal interface structure on the mechanical behavior of cu-nb fcc-bcc nano layered composites. J Mater Sci 49:6497–6516. https://doi.org/10.1007/s10853-014-8342-9

[61] Martinez E, Caro A, Beyerlein IJ (2014) Atomistic modeling of defect-induced plasticity in cunb nanocomposites. Phys Rev B 90:054103

[62] Mayeur JR, Beyerlein IJ, Bronkhorst CA, Mourad HM (2015) Incorporating interface affected zones into crystal plasticity. Int J Plast 65:206–225

[63] Mianroodi JR, Hunter A, Beyerlein IJ, Svendsen B (2016) Theoretical and computational comparison of models for dislocation dissociation and stacking fault/core formation in fcc systems. J Mech Phys Solids 95:719–741

[64] Mianroodi JR, Svendsen B (2015) Atomistically determined phase-field modeling of dislocation dissociation, stacking fault formation, dislocation slip, and reactions in fcc systems. J Mech Phys Solids 77:109–122

[65] Misra A (2006) Mechanical behavior of metallic nanolaminates. In: Hannink RHJ, Hill AJ (eds) Nanostructure control of materials, chap. 7. Woodhead Publishing Limited, Cambridge, pp 146–176

[66] Misra A, Gibala R (1999) Slip transfer and dislocation nucleation processes in multiphase ordered ni-fe-al alloys. Metall Mater Trans A 30(4):991–1001

[67] Misra A, Hirth JP, Hoagland RG (2005) Length-scale-dependent deformation mechanisms in incoherent metallic multilayered composites. Acta Mater 53(18):4817–4824

[68] Monclús MA, Zheng SJ, Mayeur JR, Beyerlein IJ, Mara NA, Polcar T, Llorca J, Molina-Aldareguía JM (2013) Optimum high temperature strength of two-dimensional nanocomposites. Appl Phys Lett Mater 1(5):052103

[69] Mura T (1987) Micromechanics of defects in solids. Kluwer Academic Publishers, Dordrecht, The Netherlands

[70] Nizolek T, Begley MR, McCabe RJ, Avallone JT, Mara NA, Beyerlein IJ, Pollock TM (2017) Strain fields induced

by kink band propagation in cu-nb nanolaminate composites. Acta Mater 133:303–315

[71] Nizolek T, Beyerlein IJ, Mara NA, Avallone JT, Pollock TM (2016) Tensile behavior and flow stress anisotropy of accumulative roll bonded cu-nb nanolaminates. Appl Phys Lett 108:051903

[72] Nizolek T, Mara NA, Beyerlein IJ, Avallone JT, Pollock TM (2014) Processing and deformation behavior of bulk cu-nb nanolaminates. Metallogr Microstruct Anal 3:470–476

[73] Ortiz M, Phillips R (1999) Nanomechanics of defects in solids. Adv Appl Mech 36:1–79

[74] Pacheco ES, Mura T (1969) Interaction between a screw dislocation and a bimetallic interface. J Mech Phys Solids 17(3):163–170

[75] Patriarca L, Abuzaid W, Sehitoglu H, Maier HJ (2013) Slip transmission in bcc fecr polycrystal. Mater Sci Eng A 588:308–317

[76] Peierls R (1940) The size of a dislocation. Proc Phys Soc 52(1):24–37

[77] Rao SI, Hazzledine PM (2000) Atomistic simulations of dislocation-interface interactions in the cu-ni multilayer system. Philos Mag A 80(9):2011–2040

[78] Roters F, Eisenlohr P, Hantcherli L, Tjahjanto DD, Bieler TR, Raabe D (2010) Overview of constitutive laws, kinematics, homogenization, and multiscale methods in crystal plasticity finite element modeling: theory, experiments, applications. Acta Mater 58(4):1152–1211

[79] Ruffini A, Le Bouar Y, Finel A (2017) Three-dimensional phase-field model of dislocations for a heterogeneous face-centered cubic crystal. J Mech Phys Solids 105:95–115

[80] Schweitz KO, Chevallier J, B J, Matz W, Schell N (2001) Hardness in ag/ni au/ni and cu/ni multilayers. Philos Mag A 81(8):2021–2032

[81] Seal JR, Crimp MA, Bieler TR, Boehlert CJ (2012) Analysis of slip transfer and deformation behavior across the α/β interface in ti-5al-2.5 sn (wt.%) with an equiaxed microstructure. Mater Sci Eng A 552:61–68

[82] Shehadeh MA, Lu G, Banerjee S, Kioussis N, Ghoniem N (2007) Dislocation transmission across the cu/ni interface: a hybrid atomistic-continuum study. Philos Mag 87(10):1513–1529

[83] Shen C, Wang Y (2004) Incorporation of γ-surface to phase field model of dislocation:simulating dislocation dissociation in fcc crystals. Acta Mater 52:683–691

[84] Shen Y, Anderson PM (2006) Transmission of a screw dislocation across a coherent, slipping interface. Acta Mater 54:3941–3951

[85] Shen Y, Anderson PM (2007) Transmission of a screw dislocation across a coherent, non-slipping interface. J Mech Phys Solids 55:956–979

[86] Subedi S, Beyerlein IJ, LeSar R, Rollet AD (2018) Strength of nanoscale metallic multilayers. Scr Mater 145:132–136

[87] Szajewski BA, Hunter A, Beyerlein IJ (2017) The core structure and recombination energy of a copper screw dislocation: a peierls study. Philos Mag 97(3):2143–2163

[88] Szajewski BA, Hunter A, Luscher DJ, Beyerlein IJ The influence of anisotropy on the core structure of shockley partial dislocations within fcc materials. Model Simul Mater Sci Eng. http://iopscience.iop.org/10.1088/1361-651X/aa9758

[89] Voyiadjis GZ, Faghihi D, Zhang Y (2014) A theory for grain boundaries with strain-gradient plasticity. Int J Solids Struct 51(10):1872–1889

[90] Wang J, Beyerlein IJ, Mara NA, Bhattacharyya D (2011) Interface-facilitated deformation twinning in copper within submicron ag-cu multilayered composites. Scr Mater 64(12):1083–1086

[91] Wang J, Hoagland RG, Hirth JP, Misra A (2008) Atomistic modeling of the interaction of glide dislocations with weak interfaces. Acta Mater 56(19):5685–5693

[92] Wang J, Zhang RF, Zhou CZ, Beyerlein IJ, Misra A (2014) Interface dislocation patterns and dislocation nucleation in face-centered-cubic and body-centered-cubic bicrystal interfaces. Int J Plast 53:40–55

[93] Wang L, Eisenlohr P, Yang Y, Bieler TR, Crimp MA (2010) Nucleation of paired twins at grain boundaries in titanium. Scr Metall 63(4):827–830

[94] Wang L, Yang Y, Eisenlohr P, Bieler TR, Crimp MA, Mason DE (2010) Twin nucleation by slip transfer across grain boundaries in commercial purity titanium. Metall Mater Trans A 41(2):421–430

[95] Wang YU, Jin YM, Cuitiño AM, Khachaturyan AG (2001) Nanoscale phase field microelasticity theory of dislocations: model and 3d simulations. Acta Mater 49:1847–1857

[96] Wang ZQ, Beyerlein IJ (2011) An atomistically-informed dislocation dynamics model for the plastic anisotropy and tension-compression asymmetry of bcc metals. Int J Plast 27(10):1471–1484

[97] Wang ZQ, Beyerlein IJ, LeSar R (2009) Plastic anisotropy of fcc single crystals in high rate deformation. Int J Plast 25:26–48

[98] Werner E, Prantl W (1990) Slip transfer across grain and phase boundaries. Acta Metall Mater 38(3):533–537

[99] Werner E, Stüwe HP (1985) On the work-hardening of dual-phase alloys. Z Metall 76(5):353–357

[100] Werner E, Stüwe HP (1985) Phase boundaries as obstacles to dislocation motion. Mater Sci Eng 68(2):175–182

[101] Zbib HM, Overman CT, Akasheh F, Bahr D (2011) Analysis of plastic deformation in nanoscale metallic multilayers with coherent and incoherent interfaces. Int J Plast 27(10):1618–1639

[102] Zeng Y, Hunter A, Beyerlein IJ, Koslowski M (2016) A phase field dislocation dynamics model for a bicrystal interface system: an investigation into dislocation slip transmission across cube-on-cube interfaces. Int J Plast 79:293–313

[103] Zhang RF, Germann TC, Liu J, Wang J, Beyerlein IJ (2014) Layer size effect on the shock compression behavior of fcc-bcc nanolaminates. Acta Mater 79:74–83

[104] Zheng S, Beyerlein IJ, Carpenter JS, Kang K, Wang J, Han W, Mara N (2013) High-strength and thermally stable bulk nanolayered composites due to twin-induced interfaces. Nat Commun 4(1696):1–8

[105] Zheng S, Ni Y, He L (2015) Phase field modeling of a glide dislocation transmission across a coherent sliding interface. Model Simul Mater Sci Eng 23:035002